

Deformation behaviors of three-dimensional auxetic spacer fabrics

Zhengyue Wang, Hong Hu and Xueliang Xiao

Textile Research Journal published online 21 February 2014

DOI: 10.1177/0040517514521120

The online version of this article can be found at:

<http://trj.sagepub.com/content/early/2014/02/20/0040517514521120>

Published by:



<http://www.sagepublications.com>

Additional services and information for *Textile Research Journal* can be found at:

Email Alerts: <http://trj.sagepub.com/cgi/alerts>

Subscriptions: <http://trj.sagepub.com/subscriptions>

Reprints: <http://www.sagepub.com/journalsReprints.nav>

Permissions: <http://www.sagepub.com/journalsPermissions.nav>

>> [OnlineFirst Version of Record](#) - Feb 21, 2014

[What is This?](#)

Deformation behaviors of three-dimensional auxetic spacer fabrics

Zhengyue Wang, Hong Hu and Xueliang Xiao

Textile Research Journal

0(00) 1–12

© The Author(s) 2014

Reprints and permissions:

sagepub.co.uk/journalsPermissions.nav

DOI: 10.1177/0040517514521120

trj.sagepub.com



Abstract

Auxetic spacer fabrics are a novel kind of three-dimensional (3D) fabric structure with a negative Poisson's ratio. They have found a number of applications in functional garments, protective pads and sportive shoes due to their unusual properties. In this paper, a study on deformation behaviors of 3D spacer fabrics that could be fabricated on a large scale is reported. Through experimental observations of deformation of a basic hexagonal unit at different tensile strains, two different geometrical models are proposed for the fabric structure when extended in the course direction and wale direction, respectively. Based on the geometrical models, two semi-empirical equations between the Poisson's ratio and tensile strain are established for both tensile directions. The study shows that the established semi-empirical equations fit well with experimental results. Therefore, they could be used in the design and prediction of 3D auxetic spacer fabrics with different values of geometrical parameters.

Keywords

auxetic material, negative Poisson's ratio, warp knitting, spacer fabric, deformation behavior

Auxetic fabrics are a kind of textile structure with a negative Poisson's ratio (PR).^{1,2} They laterally expand when stretched or laterally shrink when compressed. This unusual behavior makes them very interesting in many applications, such as functional garments, health care, protective clothing and so on, due to a number of fascinating properties, such as enhanced porosity under extension, excellent formability to curved surfaces, high energy absorption ability, etc.²

Although auxetic fabrics only represent a small part of auxetic materials,³ an increasing attention has been paid to them by various researchers in recent years. Two approaches could be adopted to fabricate auxetic fabrics. The first one is to use auxetic fibers^{4,5} or auxetic yarns^{6,7} to create auxetic behavior in a fabric structure. This approach is not widely used as there are limited auxetic fibers and yarns. Besides, auxetic behavior of yarns could be limited by fabric structure. The second one is to directly fabricate auxetic fabrics from non-auxetic fibers based on the special geometrical arrangement of yarns in a fabric structure. This approach is widely used as there is no limit in fiber materials and fabric structures. Since the geometry arrangement is

the key point to achieve the auxetic behavior of fabric in this approach, the selection of a suitable textile technology to produce desired auxetic fabric structures is very important. So far, most auxetic fabrics are produced through knitting technology, since knitting technology is very suitable to knit the required geometrical structures for obtaining auxetic behavior. Ugbole et al.^{8,9} first designed and fabricated a series of open warp-knitted fabrics based on reentrant structures. However, auxetic behavior of these fabrics was difficult to maintain due to very low structural stability and low elastic recovery ability. Alderson et al.¹⁰ developed another group of warp-knitted auxetic fabrics based on a double arrowhead geometrical configuration using

Institute of Textiles and Clothing, The Hong Kong Polytechnic University, Hong Kong

Corresponding author:

Hong Hu, Institute of Textiles and Clothing, The Hong Kong Polytechnic University, Hung Hom, Hong Kong.

Email: tchuhong@polyu.edu.hk

two kinds of fibers with different mechanical properties. It was found that the auxetic effect was only achieved when extended in the diagonal directions of the fabric. In addition to warp-knitted auxetic fabrics, weft-knitted fabrics were also developed by other researchers using flat knitting technology. Liu et al.¹¹ fabricated a special kind of weft-knitted fabric based on an origami structure that was formed with connected parallelograms. A geometrical model was also proposed by them to theoretically calculate the PR values of these fabrics. According to their study, the lowest PR obtained of these fabrics could reach -0.6 . Hu et al.¹² developed another series of weft-knitted auxetic fabrics based on different geometrical configurations, such as folded structures, rotating squares and reentrant hexagons. These fabrics could create special design effects for knitwear design.

One of the drawbacks of auxetic knitted structures is their low modulus and strength, which limit their application in the engineering field. Therefore, auxetic fabrics produced through other textile technologies were also proposed. Ge and Hu¹³ and Ge et al.¹⁴ recently developed a novel kind of three-dimensional (3D) auxetic fabric structure for composite reinforcement by using a special machine built based on a combination of non-woven and stitching technologies.¹⁵ The structure is very suitable for producing composite materials for impact protection as it can laterally contract when compressed along its thickness direction, resulting in a unique feature in that the material can concentrate itself under impacting load.¹⁶

Although a lot of auxetic fabrics have been successfully developed, their production and application are still very limited. To overcome this obstacle, a new method has recently been proposed to produce a new kind of 3D auxetic fabric on a large scale based on a warp-knitted spacer structure.^{17,18} Spacer fabrics have found many good applications, such as sportswear,¹⁹ medical care²⁰ and sound absorption.²¹ There is no doubt that the spacer fabrics with auxetic behavior will make them more attractive for these applications. Actually, a number of practical applications, such as functional garments, protective pads and sportive shoes, have been found for auxetic spacer fabrics, and an industrial production machine is being built in order to produce this kind of 3D auxetic spacer fabric on an industrial scale to meet a real requirement of the market for auxetic fabrics. A study has shown that this kind of fabric has the in-plane auxetic effect in all directions,¹⁸ and the lowest negative PR could reach -2.5 . Although the previous study could provide some useful information on 3D auxetic spacer fabrics, the relationships between the geometrical parameters of the fabric structure and the deformation behavior are still unknown. In this

paper, a further study to establish these relationships is presented, since they are very important in the design and prediction of auxetic behavior of the fabrics for required applications.

Experimental details

Fabric design and fabrication

As shown in Figure 1(a), auxetic spacer fabrics were designed and fabricated based on a warp-knitted spacer fabric structure in which two outer fabric layers are connected together by a group of spacer yarns to form a middle layer. Different from conventional spacer fabrics, a special geometrical arrangement of yarns in the outer layers, as shown in Figure 1(b), was designed to achieve auxetic behavior of the spacer fabric structure. The arrows located at the left-lower corner in Figure 1(b) indicate the course and wale directions of the fabric structure. A basic unit of the surface structure is shown in Figure 1(c). It is a deformed hexagon constructed with two different lengths of ribs that are represented by different thicknesses of lines. It can be seen that the short ribs are presented by thin lines, and the long ribs are represented by thick lines. As shown in Figure 1(c), the geometrical parameters, including the length of the short rib l_0 , the length of the long rib L_0 , the angle of the long rib formed with the vertical line α_0 , and the angle of the short rib formed with the vertical line β_0 , are sufficient to determine the geometrical feature of the structure at the initial state. For fabricating the designed fabrics, the base hexagonal spacer fabrics were firstly knitted on a double warp knitting machine equipped with six yarn-guide bars, and then the fabrics were treated with a heat-setting process to fix their geometrical configuration as designed. In this study, the base hexagonal spacer fabric was knitted using 0.12 mm (15.6 tex) polyester monofilament as the middle layer and 400D/96F polyester DTY as two outer layers according to the chain notations, as shown in Table 1. After treatment, three auxetic fabrics with different initial angles were obtained, that is, Fabrics A, B and C. To determine the parameters of each auxetic fabric, as shown in Figure 1(d), the outlines of the ribs of the hexagon are depicted on the original photos. To reduce the testing error, the outline of six hexagons in three adjacent rows and two adjacent columns are depicted. The lengths of the long rib (L_0), short rib (l_0) and the angle α_0 , β_0 were measured with the screen ruler and screen protractor. Then the lengths of the ribs were converted to the real lengths by the proportional scale. The mean values of the ribs and angles calculated are listed in Table 1.

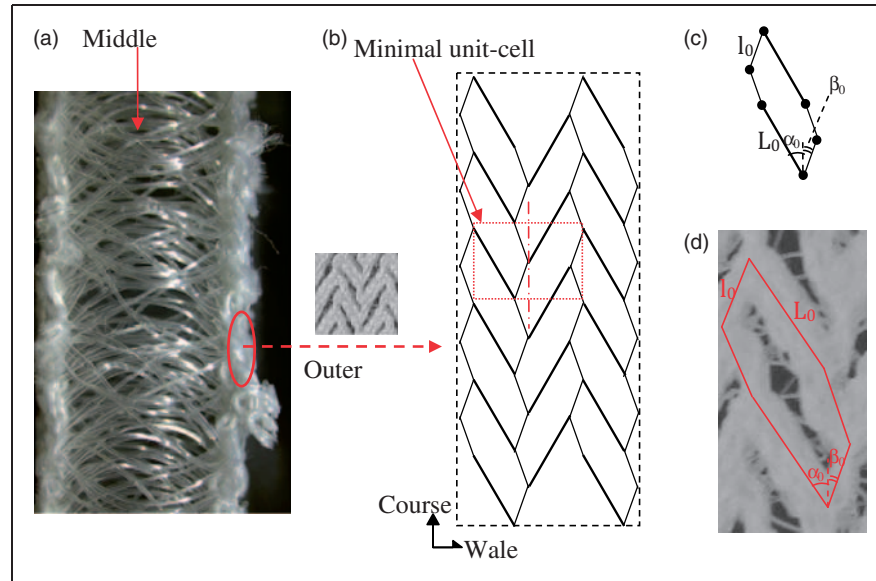


Figure 1. Three-dimensional auxetic spacer fabric structure: (a) cross-section; (b) geometrical configuration of outer fabric layers; (c) hexagon unit; (d) outline of hexagon unit.

Table 1. Geometrical parameters of three-dimensional auxetic spacer fabrics fabricated

Fabric	L_0 (cm)	l_0 (cm)	α_0 (degree)	β_0 (degree)
Fabric A	0.44	0.220	32	23
Fabric B	0.44	0.222	36	30
Fabric C	0.44	0.224	40	32
Chain notation of fabrics	GB1: (1-0-0-0/1-2-2-2)*3/(2-3-3-3/2-1-1-1)*3//			
	GB2: (2-3-3-3/2-1-1-1)*3/(1-0-0-0/1-2-2-2)*3//			
	GB3: 4-5-4-3/4-5-4-3/4-5-4-3/4-5-4-3/4-5-4-3/4-5-3-2/3-4-3-2/3-4-3-2/3-4-3-2/3-4-3-2/4-5-4-3//			
	GB4: 1-0-1-2/1-0-1-2/1-0-1-2/1-0-1-2/1-0-1-2/1-0-2-3/2-1-2-3/2-1-2-3/2-1-2-3/2-1-2-3/1-0-1-2//			
	GB5: (2-3-3-3/2-1-1-1)*3/(1-0-0-0/1-2-2-2)*3//			
	GB6: (1-0-0-0/1-2-2-2)*3/(2-3-3-3/2-1-1-1)*3//			

Tensile tests

In order to investigate the deformation behavior of these auxetic spacer fabrics, a series of uni-axial tensile tests were conducted on an INSTRON 5566 tensile machine by using a load cell of 10 kN. Because of anisotropic behavior of the fabric structure, the tensile tests were carried out in the course direction and wale direction of the fabrics, respectively. The gauge length and testing speed of the machine were set at 150 mm and 30 mm/min, respectively.

In order to see how the geometry of the fabric outer layers is deformed under extension, a hexagonal unit was observed and its photos were taken by a high-resolution camera (Cannon G10 and connected with a computer for timer shot control) at an interval of every 10% tensile strain. As the monofilaments in the

middle layer of the fabric are almost oriented in the thickness direction, which is perpendicular to the tensile direction, they mainly affect the thickness change of the fabric and their effect on the in-plane deformation of the outer structure is relatively small. Therefore, only the deformation of outer layers was observed and analyzed.

In addition to the observation of deformation of the hexagonal unit, the size changes in both the tensile and transversal directions of the fabrics were also recorded for calculating their PR values for given tensile strains. To do that, nine points were marked on the sample, as shown in Figure 2. The same camera, having a timer shot function, was used to capture the pictures of the sample at an interval of every 6 seconds. As shown in Figure 2, in order to facilitate the measurement, the nine points were marked on the central part of each

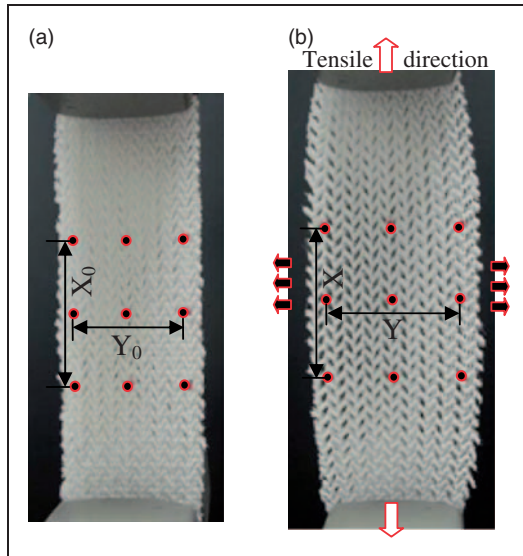


Figure 2. Points marked on an auxetic fabric sample: (a) initial state; (b) extended state.

fabric sample. The central point was used as the reference point for depicting other points, and it was not used in the measurement. A photo for each fabric sample was firstly taken before testing in order to get the original length (X_0) and width (Y_0) of the fabric. Then other photos were taken during testing to get the length (X) and width (Y) at each time interval. Three pairs of dots in the tensile direction were measured and the mean value was obtained as the value of X . While in the transverse direction, only the middle pair of dots was measured as the value of Y because the other two pairs of dots were affected by the boundary condition of two clamped ends. The measured values were finally used to calculate the tensile and transverse strains through Equations (1) and (2):

$$\varepsilon_a = -\frac{X - X_0}{X_0} \quad (1)$$

$$\varepsilon_t = -\frac{Y - Y_0}{Y_0} \quad (2)$$

After the tensile strain ε_a and transversal strain ε_t were known, PR ν was calculated through Equation (3):

$$\nu = -\frac{\varepsilon_t}{\varepsilon_a} \quad (3)$$

In order to determine a suitable sample size, the samples of Fabric A with three different sizes, 200 mm × 100 mm, 200 mm × 50 mm and 200 mm × 25 mm, were firstly tested. The largest sample width

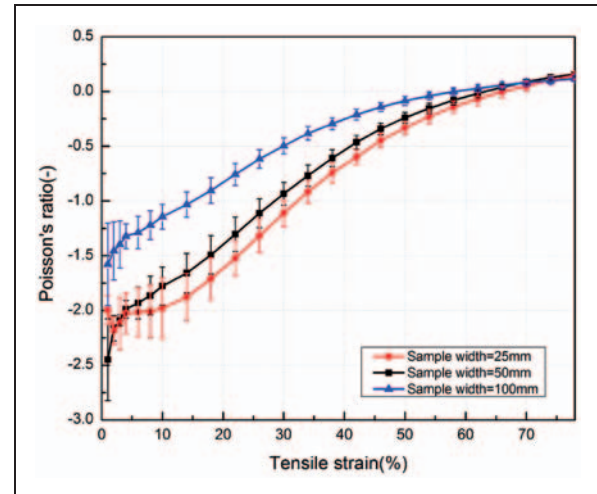


Figure 3. Poisson's ratio–strain curves of Fabric A when extended in the course direction with different fabric sample widths.

was selected as 100 mm due to the limitation of the largest size of the clamps, and the narrowest sample width was selected as 25 mm to ensure there were adequate unit-cells in the width direction. The PR-strain curves when stretched in the course and wale directions were plotted and are shown in Figures 3 and 4, respectively.

Theoretically, since the same fabric has the same unit-cell structure, the tensile behavior should be the same and the same PR-strain curve with different sample sizes should be obtained. However, in the real test, the fabric deformation is affected by the boundary conditions. As shown in Figure 5(a), the two clamped ends of the fabric restrict its expansion in the transversal direction. The larger the sample width, the higher restriction the clamps have. For extension in the wale direction, as the width change is small during testing (Figure 5(b)), the boundary effect is not evident. Therefore, the PR-strain curves obtained with different sample sizes are more closed (Figure 4). However, as shown in Figure 3, more difference exists among the PR-strain curves obtained with different sample sizes when extended in the course direction. The sample in the width of 100 mm has lower negative PR values as the clamps restrict more expansion of the fabric in the transversal direction. For the samples with 50 and 25 mm widths, their PR-strain curves are closed, but it can be found that the PR-strain curve of the sample with 25 mm width is not regular in the initial stage of testing. The reason is that the narrower sample is more easily affected by the fabric edges in the tensile direction and may cause more measurement errors. As the samples with too large width and too narrow width are not suitable, 50 mm was selected as the sample width in this study.

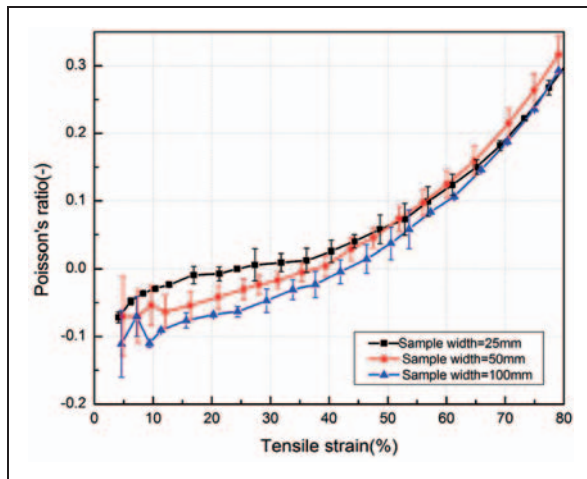


Figure 4. Poisson's ratio–strain curves of Fabric A when extended in the warp direction with different fabric sample widths.

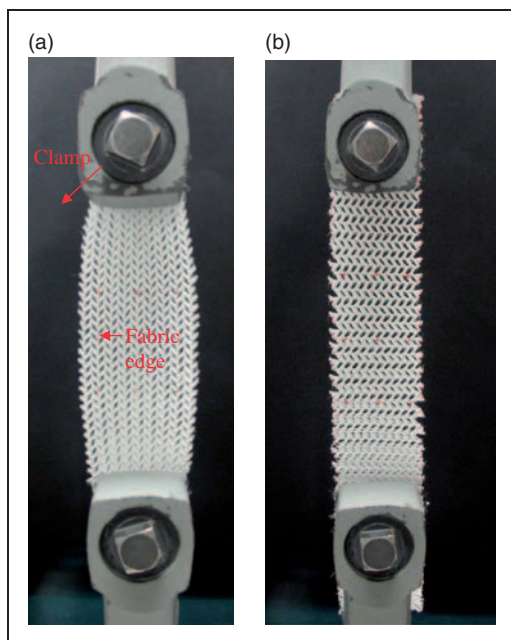


Figure 5. Clamp restriction: (a) extended in the course direction; (b) extended in the wale direction.

Results and discussion

As 3D auxetic fabrics fabricated have an anisotropic structure, their deformation behavior in each tensile direction should be different. In this study, only the deformation behaviors of the fabrics in the course and wale directions were investigated, as these two directions are the main directions of the fabrics. The study was the first to experimentally observe the deformation of a hexagonal unit when extended in the course and

wale directions, respectively. Based on the assumptions made from the observations, the geometrical model in each tensile direction was proposed. The relation between the PR and tensile strain for each tensile direction was then established through the analysis of the geometrical model. With use of the established relation, the deformation behavior of the fabric structure in each tensile direction could be finally predicted for different values of geometrical parameters.

Deformation behavior when extended in the course direction

Experimental observation. The photos of a hexagonal unit taken at different tensile strains when extended in the course direction of Fabric A are shown in Figure 6. For a better observation, all the photos were magnified by eight times. As the fabric consists of contiguous hexagons, the observation of a hexagon unit is sufficient for analyzing the deformation behavior of the structure. However, it should be noted that the hexagon unit is not the minimal unit-cell. The minimal unit-cell of the fabric structure is outlined by a rectangle, as shown in Figure 1(b). Since the minimal unit-cell has the symmetrical deformation effect along the central line, the half unit-cell is enough for calculating the PR, as shown in Figure 6. For the short ribs, it can be seen that they are firstly straightened and then extended in the tensile direction. Therefore, the tensile strain is mainly dependent on the length change of short ribs. For the long ribs, it can be seen that they firstly rotate along the anti-clockwise direction, and then shrink. While the rotation of the long ribs to the horizontal direction can increase the transversal strain of the structure, shrinking of the long ribs can lead to a decrease of the transversal strain. Therefore, the transverse strain is mainly dependent on a combination effect of the length change and rotation of the long ribs. From the observation, it can also be noted that the transversal size of the hexagonal unit first increases and then decreases with the increase of tensile strain. When the fabric transversal size becomes smaller than its initial size, the PR of the fabric structure changes from negative to positive.

Comparing all the photos in Figure 6, it is noted that the deformation of a hexagonal unit when extended in the course direction is like the deformation of a parallelogram, as shown in Figure 7. Therefore, a parallelogram geometric model is proposed in the following to help analyze the deformation behavior of the auxetic fabric structure when extended in the course direction.

Geometric analysis. The main objective of the geometrical analysis is to establish the relation between the PR and

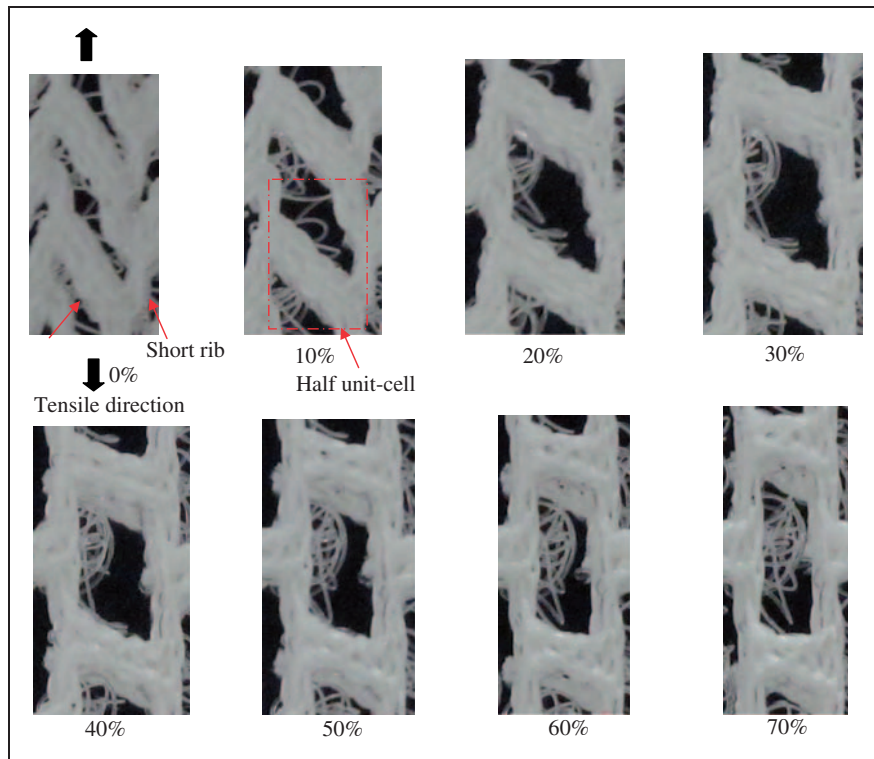


Figure 6. Photos of a hexagonal unit of Fabric A taken at different tensile strains in the course direction.

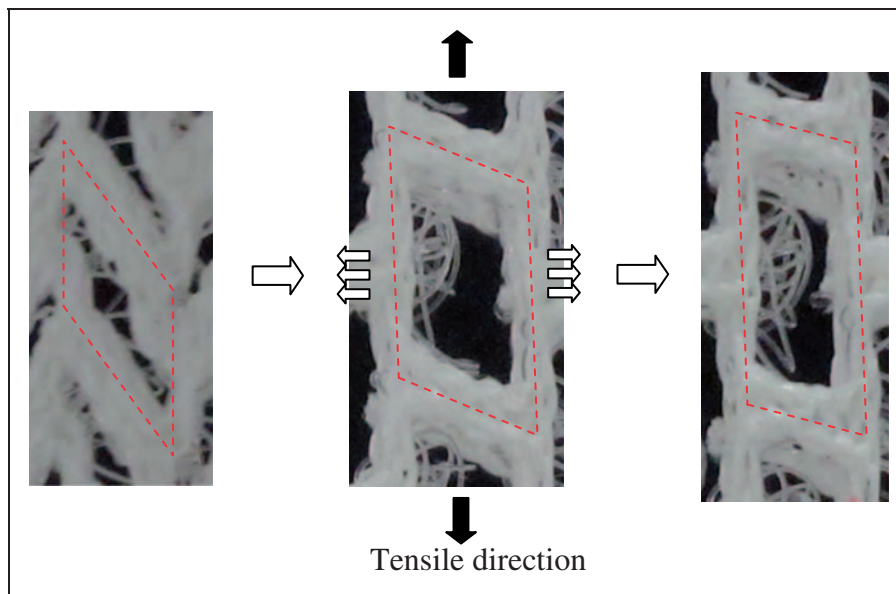


Figure 7. Representation of a hexagonal unit of Fabric A by a parallelogram.

tensile strain of the structure. To simplify the analysis, the following assumptions are first made.

1. All the hexagonal units have the same shape and size at the initial state. They will have the same deformation behavior under extension.

2. The deformation of a hexagonal unit can be represented by deformation of an equivalent parallelogram.

The geometric model proposed is shown in Figure 8. From Figure 8(a), it can be seen that the angle of two

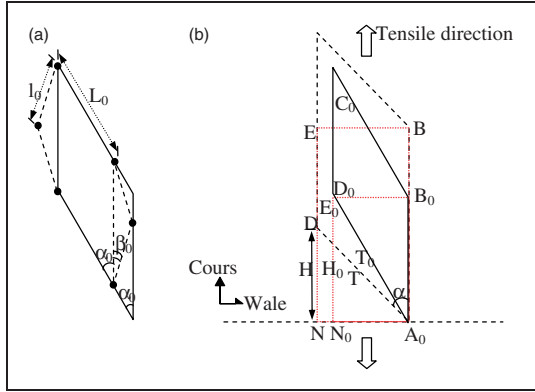


Figure 8. Geometric model in the course direction: (a) representation of the hexagonal unit by an equivalent parallelogram; (b) deformation of the parallelogram under extension.

sides of the parallelogram at its right-lower corner equals the angle of the long rib formed with the vertical line α_0 . This condition is used in the following geometrical analysis. From Figure 8(b), it can be seen that under extension in the course direction, the initial parallelogram $A_0B_0C_0D_0$ is deformed to the parallelogram A_0BCD , and the half unit-cell $A_0B_0E_0N_0$ is changed to rectangle A_0BEN . For ease of writing, it is supposed that $A_0D_0 = T_0$, $A_0D = T$, $D_0N_0 = H_0$ and $DN = H$.

Due to the complicated changes in the long ribs and short ribs during extension, it is very difficult to theoretically determine the change of T and H , as shown in Figure 8(b). However, from the photos shown in Figure 6, it is easy to determine their change trends. Figure 9 shows the variation trends of T and H as a function of tensile strain obtained through the picture analysis of the photos shown in Figure 6. It can be found that T has a power trend, while H has a linear trend. Based on these trends, the following assumptions defined by Equations (4) and (5) are further made:

$$T = T_0(1 + a_1 * \varepsilon_a^{b_1}) \quad (4)$$

$$H = H_0(1 + a_2 * \varepsilon_a) \quad (5)$$

where ε_a is the tensile strain of the fabric structure when extended in the course direction and a_1 , b_1 and a_2 are constants that could be determined from experimental results. Then the transverse strain ε_t can be derived as Equation (6):

$$\begin{aligned} \varepsilon_t &= \frac{NA_0 - N_0A_0}{N_0A_0} = \frac{\sqrt{T^2 - H^2} - T_0 * \sin \alpha_0}{T_0 * \sin \alpha_0} \\ &= \frac{\sqrt{T_0^2(1 + a_1 * \varepsilon_a^{b_1})^2 - H_0^2(1 + a_2 * \varepsilon_a)^2} - T_0 * \sin \alpha_0}{T_0 * \sin \alpha_0} \end{aligned} \quad (6)$$

Through the geometrical analysis, the relationship between T_0 and H_0 can be obtained, and is given by Equation (7):

$$H_0 = T_0 * \cos \alpha_0 \quad (7)$$

Substituting Equation (7) into Equation (6) gives Equation (8):

$$\begin{aligned} \varepsilon_t &= \frac{\sqrt{T_0^2(1 + a_1 * \varepsilon_a^{b_1})^2 - T_0^2 * (\cos \alpha_0)^2 * (1 + a_2 * \varepsilon_a)^2} - T_0 * \sin \alpha_0}{T_0 * \sin \alpha_0} \\ &= \frac{\sqrt{(1 + a_1 * \varepsilon_a^{b_1})^2 - (\cos \alpha_0)^2 * (1 + a_2 * \varepsilon_a)^2} - \sin \alpha_0}{\sin \alpha_0} \end{aligned} \quad (8)$$

By substituting Equation (8) into Equation (3), Equation (9), which defines the relation between the PR and tensile strain when extended in the course direction, is obtained:

$$v = -\frac{\varepsilon_t}{\varepsilon_a} = \frac{\sin \alpha_0 - \sqrt{(1 + a_1 * \varepsilon_a^{b_1})^2 - (\cos \alpha_0)^2 * (1 + a_2 * \varepsilon_a)^2}}{\varepsilon_a * \sin \alpha_0} \quad (9)$$

From Equation (9), it can be found that there are three constants a_1 , b_1 and a_2 needing to be determined. Here the experimental relationship between the PR and tensile strain of Fabric A is used to determine these constants. Both the calculated curve and experimental values are shown in Figure 10. It can be seen that the calculated curve fits well with experimental results.

Fitting Equation (9) with the experimental results of Fabric A gives $a_1 = -0.83$, $b_1 = 1.73$ and $a_2 = -1$. Substituting these values into Equation (9) gives Equation (10), which is a semi-empirical equation for theoretically calculating the PR of the structure when the tensile strain in the course direction is given:

$$v = \frac{\sin \alpha_0 - \sqrt{(1 - 0.83 * \varepsilon_a^{1.73})^2 - (\cos \alpha_0)^2 * (1 - \varepsilon_a)^2}}{\varepsilon_a * \sin \alpha_0} \quad (10)$$

Verification and prediction. To verify the validation of Equation (10), the testing results of the other two fabric samples (Fabric B and Fabric C) made with different values of α_0 are compared to the curves plotted with Equation (10). The comparisons are shown in Figure 11. It can be seen that the calculated curves fit well with experimental results. Therefore, Equation (10)

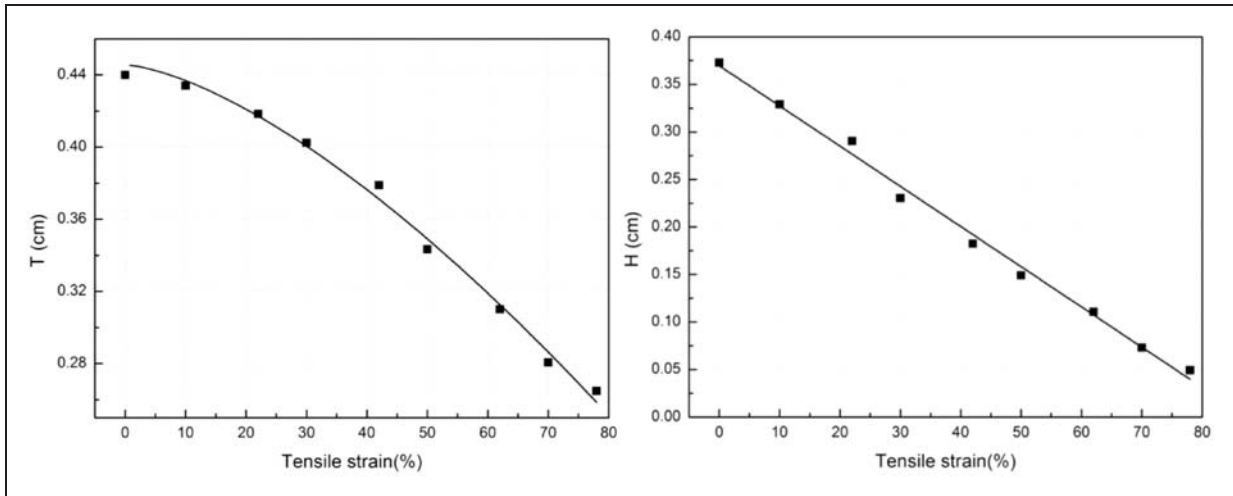


Figure 9. Variation trends of T and H as a function of tensile strain.

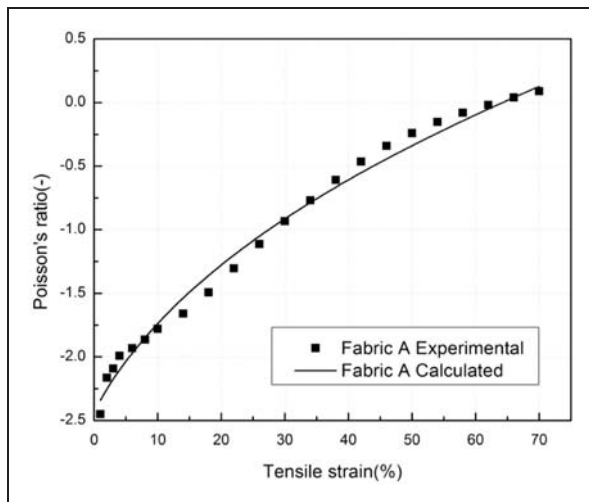


Figure 10. Curve fitted with experimental values when extended in the course direction.

is validated and can be used to predict the PR of auxetic spacer fabrics that are knitted with the same yarns, the same geometrical parameters L_0 and l_0 and the same machine gauge as Fabric A, but with different α_0 and β_0 . From Equation (10), it can also be seen that the PR of the fabric structure when extended in the course direction only depends on α_0 . In order to know how α_0 affects the PR of 3D auxetic spacer fabric structure, the PR curves as a function of the tensile strain are plotted for different values of α_0 by using Equation (10), as shown in Figure 12. It can be seen that the auxetic behavior, that is, negative PR value, of the auxetic spacer fabric structure rapidly increases with the decrease of α_0 . This phenomenon can be explained by

the fact that the decrease of α_0 makes the fabric structure closer and easier to be opened under extension, leading to a higher deformation in the transversal direction. Therefore, to design an auxetic spacer fabric with high negative PR when extended in the course direction, a small α_0 should be used.

Deformation behavior when extended in the wale direction

Experimental observation. The deformations of a hexagonal unit when extended in the wale direction of Fabric A are shown in Figure 13. The photos are also magnified by eight times for better observation. The same as course direction, the half unit-cell is outlined by a rectangle. Observing these photos, it can be seen that the long ribs first rotate to the tensile direction and then are extended during extension. The short ribs are curved at the beginning. They are first straightened and then extended. They also rotate to the tensile direction during extension. Therefore, the tensile strain in the wale direction of the fabric mainly depends on the rotation and extension of both the long and short ribs. As for the transverse strain, from the unit-cell, it can be found that it is only dependent on the length change and rotation of short ribs. While the extension of short ribs increases the transversal strain, the rotation of the short ribs to the tensile direction decreases the transversal strain.

Comparing all the photos in Figure 13, it can be found that the hexagonal unit is always kept as a hexagonal form. Therefore, a hexagonal geometric model is proposed in the following to help analyzing the deformation behavior of the auxetic spacer fabric structure when extended in the wale direction.

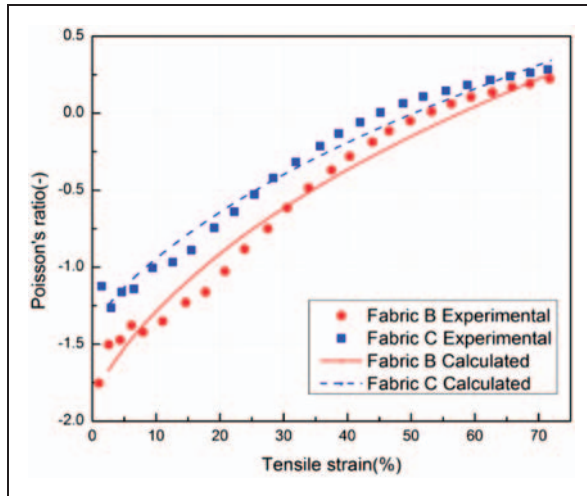


Figure 11. Comparisons between theoretically calculated curves and experimental results.

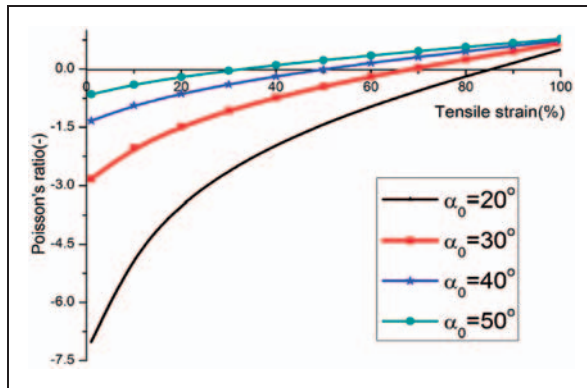


Figure 12. Effect of α_0 on Poisson's ratio of fabric structure.

Geometric analysis. For simplifying the geometric analysis, the following assumptions are first made.

1. All the hexagonal units have the same shape and size at the initial state. They will have the same deformation behavior during the extension process.
2. A hexagonal unit is always kept as a hexagonal form under extension in the wale direction.

The geometric model proposed is shown in Figure 14. While hexagon $A_0B_0C_0D_0E_0F_0$ in Figure 14(a) represents the initial state of the hexagonal unit, hexagonal $ABCDEF$ in Figure 14(b) represents the deformed state when extended in the wale direction. In each figure, the half unit-cell of the fabric structure is outlined out by a rectangle plotted with dashed lines. For easy analysis, it is supposed that $A_0B_0 = l_0$, $AB = l$, $B_0N_0 = h_0$, $BN = h$ and $\Delta A_0B_0C_0$ and ΔABC are isosceles triangles.

Due to the complicated changes in the long ribs and short ribs during the extension process, it is difficult to determine the change of l and h . However, from the photos shown in Figure 14, the variation trends of l and h can be easily determined. The variation trends of l and h as a function of tensile strain obtained through the picture analysis of the photos in Figure 14 are shown in Figure 15. It can be seen that l has a linear trend, while h has a power trend.

Based on these trends, the following assumptions defined by Equations (11) and (12) are further made:

$$l = l_0(1 + a_3 * \varepsilon_a) \quad (11)$$

$$h = h_0(1 + a_4 * \varepsilon_a^{b_4}) \quad (12)$$

where ε_a is the tensile strain of the fabric structure when extended in the wale direction and a_3 , a_4 and b_4 are constants that can be determined from experimental results. Then transverse strain ε_t can be derived and is given by Equation (13):

$$\begin{aligned} \varepsilon_t &= \frac{AC - A_0C_0}{A_0C_0} = \frac{2\sqrt{l^2 - h^2} - 2 * l_0 * \cos \beta_0}{2 * l_0 * \cos \beta_0} \\ &= \frac{\sqrt{l_0^2(1 + a_3 * \varepsilon_a)^2 - h_0^2(1 + a_4 * \varepsilon_a^{b_4})^2} - l_0 * \cos \beta_0}{l_0 * \cos \beta_0} \end{aligned} \quad (13)$$

Through the geometrical analysis, the relationship between l_0 and h_0 can be found and is given by Equation (14):

$$h_0 = l_0 * \sin \beta_0 \quad (14)$$

Substituting Equation (14) into Equation (13) gives Equation (15):

$$\begin{aligned} \varepsilon_t &= \frac{\sqrt{l_0^2(1 + a_3 * \varepsilon_a)^2 - l_0^2 * (\sin \beta_0)^2 (1 + a_4 * \varepsilon_a^{b_4})^2} - l_0 * \cos \beta_0}{l_0 * \cos \beta_0} \\ &= \frac{\sqrt{(1 + a_3 * \varepsilon_a)^2 - (\sin \beta_0)^2 (1 + a_4 * \varepsilon_a^{b_4})^2} - \cos \beta_0}{\cos \beta_0} \end{aligned} \quad (15)$$

By substituting Equation (15) into Equation (3), Equation (16), which defines the relation between the

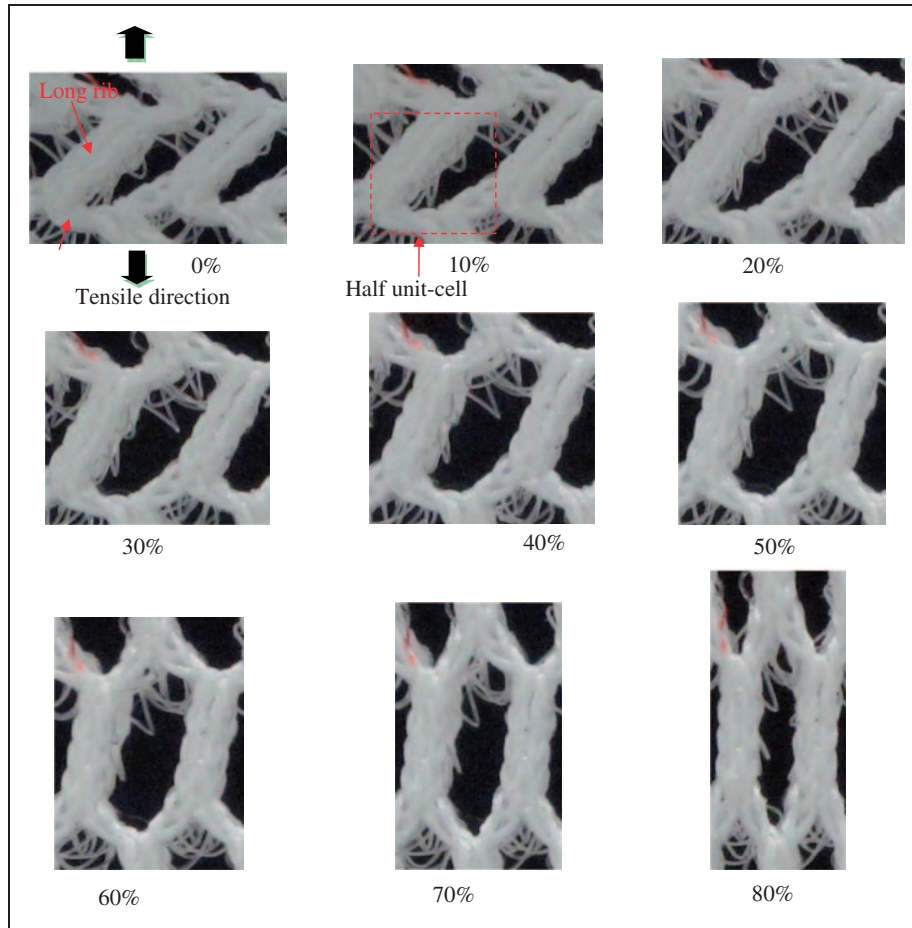


Figure 13. Photos of a hexagonal unit of Fabric A taken at different tensile strains in the wale direction.

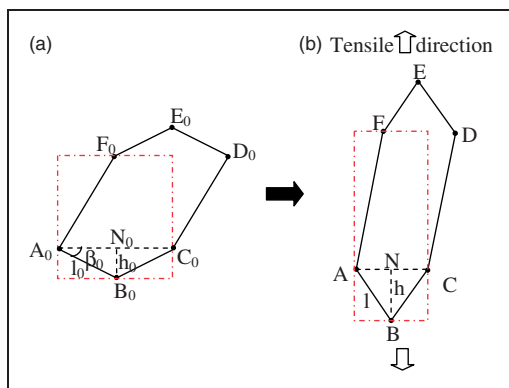


Figure 14. Geometric model in the wale direction: (a) initial state; (b) extended state.

PR and tensile strain when extended in the wale direction, is obtained:

$$v = -\frac{\epsilon_t}{\epsilon_a} = \frac{\cos \beta_0 - \sqrt{(1 + a_3 * \epsilon_a)^2 - (\sin \beta_0)^2 (1 + a_4 * \epsilon_a^{b_4})^2}}{\epsilon_a * \cos \beta_0} \tag{16}$$

From Equation (16), it can be found that there are three constants a_3 , a_4 and b_4 needing to be determined. Here the experimental relationship between the PR and tensile strain of Fabric A is used to determine these constants. Both the calculated curve and experimental values are shown in Figure 16. It can be seen that the calculated curve fits well with experimental results.

Fitting Equation (16) with the experimental data of Fabric A gives $a_3 = 0.062$, $a_4 = 1.867$, $b_4 = 2.550$. Substituting these values into Equation (16) gives Equation (17), which is a semi-empirical equation for theoretically calculating the PR of the structure when the tensile strain in the wale direction is given:

$$v = \frac{\cos \beta_0 - \sqrt{(1 + 0.062 * \epsilon_a)^2 - (\sin \beta_0)^2 (1 + 1.867 * \epsilon_a^{2.55})^2}}{\epsilon_a * \cos \beta_0} \tag{17}$$

Verification and prediction. To verify the validation of Equation (17), the testing results of the other two

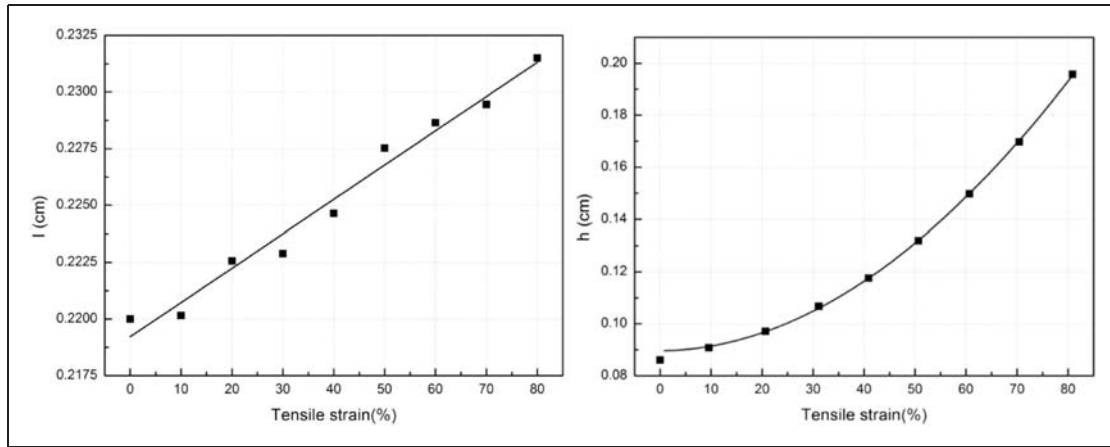


Figure 15. Variation trends of l and h as a function of tensile strain.

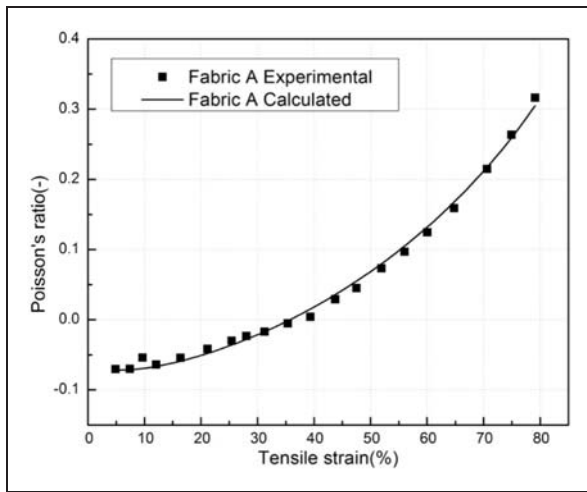


Figure 16. Curve fitted with experimental values when extended in the wale direction.

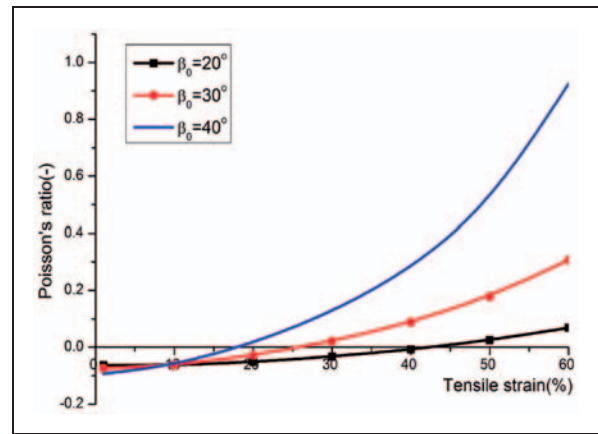


Figure 18. Effect of β_0 on Poisson's ratio of fabric structure.

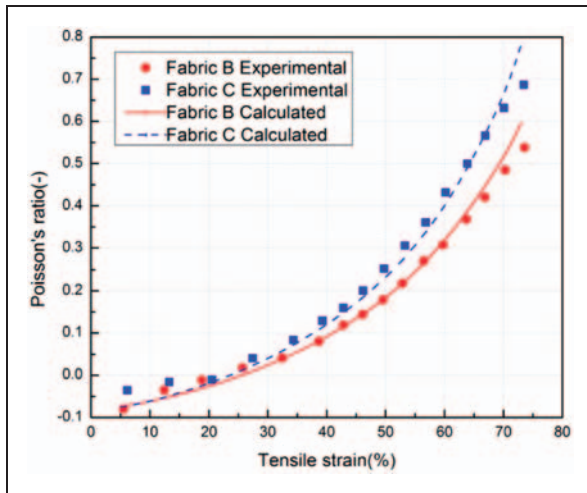


Figure 17. Comparisons between theoretically calculated curves and experimental results.

fabric samples (Fabric B and Fabric C) with different values of β_0 are compared with the curves plotted with Equation (17). The comparisons are shown in Figure 17. It can be seen that the calculated curves fit well with experimental data. Therefore, Equation (17) is validated and can be used to predict the PR of auxetic spacer fabrics that are knitted with the same yarns, the same geometrical parameters L_0 and l_0 and the same machine gauge as Fabric A, but with different α_0 and β_0 . From Equation (17), it can be also seen that the PR of the fabric structure when extended in the wale direction only depends on β_0 . In order to know how β_0 affects the PR of 3D auxetic spacer fabric structures, the PR curves as a function of the tensile strain are plotted for different values of β_0 using Equation (17), as shown in Figure 18. It can be seen that the negative PR behavior of the auxetic spacer fabric structure is not obviously affected by β_0 . However, the decrease of β_0 can increase the tensile strain range for getting auxetic behavior. It can be found that the PR becomes positive at a strain of about 17% when β_0 is 40° , and when β_0 is

20°, the strain is 40%. This is very useful when an auxetic spacer fabric is designed to have negative PR behavior in a large range of tensile strain when extended in the wale direction.

Conclusions

The deformation behaviors of 3D auxetic spacer fabric structure in both the course and wale directions were studied based on the experimental observations of a hexagonal unit and theoretical analysis of geometrical models proposed. The semi-empirical equation between the PR and tensile strain was established for each tensile direction. Some conclusions could be drawn from the study.

1. Due to the anisotropic behavior of the 3D auxetic structure, different geometrical models are needed for analyzing deformation behaviors of the structure in different tensile directions. While the deformation of the hexagonal unit in the course direction can be represented by deformation of a parallelogram, the deformation of the hexagonal unit in the wale direction always keeps in a hexagonal form.
2. Different geometrical parameters have different effects on the PR of the structure. While the PR is only affected by α_0 when extended in the course direction, it is only affected by β_0 when extended in the wale direction for fabrics having specific values of L_0 and l_0 . The increase of α_0 can lead to the decrease in the magnitude of the negative PR and the decrease of β_0 can maintain auxetic behavior in a larger range of tensile strain.
3. The semi-empirical equations obtained are simple, but fit well with experimental results. They provide a useful way for the design and prediction of 3D auxetic spacer fabrics produced with the same type of materials and same gauge of machines but with different values of geometrical parameters α_0 and β_0 .

Funding

This work was supported by the Research Grants Council of Hong Kong Special Administrative Region Government in the form of the GRF project (grant no. 518109).

References

1. Alderson A and Alderson K. Expanding materials and applications: exploiting auxetic textiles. *Tech Textil Int* 2005; 777: 29–34.
2. Wang ZY and Hu H. Auxetic materials and their potential applications in textiles. *Textil Res J*. DOI:10.1177/0040517512449051.
3. Liu YP and Hu H. A review on auxetic structures and polymeric materials. *Sci Res Essays* 2010; 5: 1052–1063.
4. Alderson KL, Alderson A, Smart G, et al. Auxetic polypropylene fibres: Part 1- manufacture and characterization. *Plast Rubber Compos* 2002; 31: 344–349.
5. Ravirala N, Alderson KL, Davies PJ, et al. Negative Poisson's ratio polyester fibers. *Textil Res J* 2006; 76: 540–546.
6. Wright JR, Sloan MR and Evans KE. Tensile properties of helical auxetic structures: a numerical study. *J Appl Phys* 2010; 108: 044905.
7. Wright JR, Burns MK, James E, et al. On the design and characterization of low-stiffness auxetic yarns and fabrics. *Textil Res J* 2012; 82: 645–654.
8. Ugbole SC, Kim YK, Warner SB, et al. The formation and performance of auxetic textiles. Part I: theoretical and technical considerations. *J Textil Inst* 2010; 101: 660–667.
9. Ugbole SC, Kim YK, Warner SB, et al. The formation and performance of auxetic textiles. Part II: geometry and structural properties. *J Textil Inst* 2011; 102: 424–433.
10. Alderson K, Alderson A, Anand S, et al. Auxetic warp knit textile structures. *Phys Status Solidi B* 2012; 249: 1322–1329.
11. Liu YP, Hu H, Lam JK, et al. Negative Poisson's ratio weft-knitted fabrics. *Textil Res J* 2010; 80: 856–863.
12. Hu H, Wang ZY and Liu S. Development of auxetic fabrics using flat knitting technology. *Textil Res J* 2011; 81: 1493–1502.
13. Ge ZY and Hu H. Innovational three-dimensional fabric structure with negative Poisson's ratio for composite reinforcement. *Textil Res J* 2013; 83: 543–550.
14. Ge Z, Hu H and Liu Y. A finite element analysis of a 3D auxetic textile structure for composite reinforcement. *Smart Mater Struct*, Special Issue on Auxetics in Smart Systems and Structures 2013; 22: 084005.
15. Hu H and Zhang ZK. *A machine for producing 3D auxetic fabric structures*. Patent application 201210192738.3, China, 2012.
16. Ge ZY and Hu H. 3D auxetic textile structure for composite reinforcement. In: *TexComp-11 conference*, Leuven, Belgium, 2013.
17. Hu H. *3D negative Poisson's ratio spacer fabric and method for making the same*. Chinese invention patent application 201210047717.2, 2012; International application PCT/CN2012/081390, 2013.
18. Wang ZY and Hu H. 3D Auxetic warp-knitted spacer fabrics. *Phys Status Solidi B*. Epub ahead of print. 20 September 2013, DOI: 10.1002/pssb.201384239.
19. Rock M and Lohmueller K. *Three-dimensional knit spacer fabric for footwear and backpacks*. Patent 5,896,758[P], USA, 1999.
20. Bagherzadeh R, Montazer M, Latifi M, et al. Evaluation of comfort properties of polyester knitted spacer fabrics finished with water repellent and antimicrobial agents. *Fiber Polym* 2007; 8: 386–392.
21. Liu Y and Hu H. Sound absorption behavior of knitted spacer fabrics. *Textil Res J* 2010; 80: 1949–1957.